A&A 482, 209–214 (2008)
DOI: 10.1051/0004-6361:20078606

Astronomy & Astrophysics

A simple way to model nebulae with distributed ionizing stars

L. Jamet and C. Morisset

Instituto de Astronomía, Universidad Nacional Autónoma de México, Apartado Postal 70-264, Ciudad Universitaria, México D.F. 04510, Mexico
e-mail: ljamet@astroscu.unam.mx

Received 3 September 2007 / Accepted 4 February 2008

ABSTRACT

Aims. This work is a follow-up of a recent article by Ercolano et al. that shows that, in some cases, the spatial dispersion of the ionizing stars in a given nebula may significantly affect its emission spectrum. The authors found that the dispersion of the ionizing stars is accompanied by a decrease in the ionization parameter, which at least partly explains the variations in the nebular spectrum. However, they did not research how other effects associated to the dispersion of the stars may contribute to those variations. Furthermore, they made use of a unique and simplified set of stellar populations. The scope of the present article is to assess whether the variation in the ionization parameter is the dominant effect in the dependence of the nebular spectrum on the distribution of its ionizing stars. We examined this possibility for various regimes of metallicity and age. We also investigated a way to model the distribution of the ionizing sources so as to bypass expensive calculations.
Methods. We wrote a code able to generate random stellar populations and to compute the emission spectra of their associated nebulae through the widespread photoionization code CLOUDY. This code can process two kinds of spatial distributions of the stars: one where all the stars are concentrated at one point, and one where their separation is such that their Strömgren spheres do not overlap.
Results. We found that, in most regimes of stellar population ages and gas metallicities, the dependence of the ionization parameter on the distribution of the stars is the dominant factor in the variation of the main nebular diagnostics with this distribution. We derived a method to mimic those effects with a single calculation that makes use of the common assumptions of a central source and a spherical nebula, in the case of constant density objects. This represents a computation time saving by a factor of at least several dozen in the case of H II regions ionized by massive clusters.

Key words. ISM: HII regions – ISM: abundances – stars: abundances

1. Introduction

So far, H II regions have been the most popular tracers of chemical elements in galaxies ranging from the Galaxy to high-redshift objects. Their highly contrasted emission lines and the supposedly simple physical processes that govern them make it easy to derive their chemical composition from spectroscopic observations. Particularly, several methods have been developed to determine the heavy element content of those objects using only the strongest lines, so that chemical composition measurements can be applied to large surveys and faint galaxies. These empirical methods are calibrated on well-observed H II regions in which the temperature could be inferred from faint lines. Hence, for the strong-line methods to be reliable, it is important to fully understand the physics of H II regions, especially their temperature and excitation structure. This purpose can be achieved only by analyzing well-observed H II regions with detailed models.

A complication arises from the fact that, historically, nearly all the models of ionized nebulae have assumed plane-parallel or spherical symmetry of the gas, with the excitation source being respectively plane or punctual. This strong simplification is needed to make carrying out numerical models with common computational resources possible. However, it is evident from images that the vast majority of H II regions are highly asymmetric, meaning that simple geometries of the gas are unrealistic in their description. Moreover, when the ionizing source of an H II region is composed of various stars, the latter are most often distributed inside the ionized gas (see, e.g., NGC 2363: Drissen et al. 2000), so plane or point-like sources are not realistic descriptions either. More sophisticated codes, and in particular fully three-dimensional ones like MOCASSIN (Ercolano 2003), are able to treat asymmetric nebulae but require computational power that was long inaccessible and is still very high even by today's standards. Hence, it is important to assess the impact of the usual simplifications on the geometry of H II regions on the prediction of the global properties of these objects, in particular the relative intensities of the emission lines.

Recently, Ercolano et al. (2007, hereafter EBS07) have explored the effects of the distribution of the ionizing stars in model nebulae. They considered very simple examples where the stellar population consisted of stars with two possible masses and where the nebula was either a full sphere or a shell, with a unique hydrogen density. They found significant differences in the emission line diagnostics between the cases where all the stars are concentrated in the center of the nebula and where they are distributed in such a way that their Strömgren spheres hardly overlap. They state that those differences arise at least partly from the dependence of the ionization parameter on the distribution of the stars. Nonetheless, other causes may also intervene, in particular the difference in the shape of the ionizing spectrum of the different stars. The purpose of the present article is to assess the relative importance of the ionization parameter in the effects noticed by EBS07 and to propose a simple way to model them, considering ranges of metallicities and stellar population ages representative of H II regions.

In Sect. 2, we describe our models. In Sect. 3, we analyze models in which the stellar populations are comparable to those

of EBS07 and propose a simple way to evaluate the impact of the dispersion of the stars on the properties of the ionized gas. In Sect. 4, we check whether this solution still stands when realistic clusters of various ages are considered. We find satisfying results except for the case of evolved clusters ionizing very metal-rich nebulae. In Sect. 5, we discuss the reasons for this peculiar failure. In Sect. 6, we propose some hints for generalizing our approach to different stellar distributions. Finally, we give our conclusions in Sect. 7.

2. The models

2.1. Ionized gas and geometry

We computed our models of ionized nebulae with version 07.02.01 of CLOUDY (Ferland et al. 1998). We considered only full spheres of gas with constant hydrogen density. We chose an outer radius large enough to ensure the nebulae were ionization-bounded, the effective stop criterion being an H^+/H abundance ratio lower than 10%. The solar values were taken from Grevesse & Sauval (1998), except for C/H (Allende Prieto et al. 2002), N/H (Holweger 2001), O/H (Allende Prieto et al. 2001), and Fe/H (Asplund 2000). We calculated the abundances at other metallicities by considering the dependence of the abundance ratios on O/H as published by Izotov et al. (2006), but using the solar values as zeropoints.

Regarding the distribution of the ionizing stars, we considered two cases: the one where all the stars are concentrated in the center of the nebula (this is the assumption of nearly all the models of nebulae carried out so far) and the one where the stars are separated in such a way that their Strömgren spheres do not overlap (the nebula is in fact an ensemble of separate H II regions, each ionized by one star). Those two configurations are equivalent to the CSp and FSp ones of EBS07, respectively; we will keep this denomination in what follows. EBS07 also computed models with an intermediate distribution of the ionizing stars (which they called HSp); this case cannot be treated with a 1D code so we did not examine it.

2.2. Stellar clusters

We considered two kinds of stellar content for the models. The first is the one used by EBS07, i.e. a population made of 1 Ma old stars whose initial masses are 37 and 56 $M_\odot$, each mass represented by the number of stars needed to produce an ionizing photon rate $Q(H^0) = 1.9 \times 10^{50}$ s^{-1}. The authors chose those masses to maximize the effects of the distribution of the stars. The second kind of stellar population, more realistic, consists of random stellar clusters. In this case, for a given cluster of metallicity Z and age τ, we drew the initial masses of N stars using the Salpeter IMF (1955) as the probability law in the range 1 $M_\odot$–$M_{\rm max}$, where $M_{\rm max}$ is the maximum initial mass possible for a star at the adopted age and metallicity. The number N was chosen to match the average one expected for a cluster of a total initial mass of 10^4 $M_\odot$.

Whichever the kind of stellar content treated, we converted the initial masses to bolometric luminosities $L_{\rm bol}$, effective temperatures $T_{\rm eff}$, surface gravities g, and stellar types using the Geneva evolutionary tracks with enhanced mass losses (Meynet et al. 1994). These tracks are available for five metallicities: $Z/Z_\odot = 0.05, 0.2, 0.4, 1$, and 2, with a solar metallicity $Z_\odot = 0.02$ for this case.

We computed the model spectra of the stars as follows. We used the stellar atmospheres of Hillier & Miller (1998) for Wolf-Rayet stars (WR), Pauldrach et al. (2001) for very hot non-WR stars, and Lejeune et al. (1997) for cooler stars. The assignment of the atmosphere grids to the stars was executed the same way as was implemented by Smith et al. (2002) in STARBURST99 (Leitherer et al. 1999). For each star, we performed a bilinear interpolation of $\log R(\nu; T_{\rm eff}, g)$ in the $(\log T_{\rm eff}, \log g)$ plane, where $R(\nu; T_{\rm eff}, g)$ is the ratio between the model spectrum at a given position of this plane and the blackbody spectrum at the same temperature and normalized to the same rate $Q(H^0)$ of ionizing photons. Finally, the spectrum for the considered star was obtained by multiplying the interpolated function $R(\nu; T_{\rm eff}, g)$ by the blackbody emission calculated at the corresponding temperature and by normalizing the resulting spectrum to match the bolometric luminosity of the star.

Among the stars drawn in a simulation (for the case of a random cluster), not all produce a significant number of ionizing photons. Hence, in a given cluster, we only kept the brightest stars in the Lyman continuum, limiting the sample to stars emitting 99% of the ionizing photons of the cluster together. Depending on the age and metallicity chosen, the number of stars selected varied from ~50 to ~90.

2.3. Manipulation of the ionizing parameter

Since we were interested in studying the impact of the ionization parameter U on the properties of our model nebulae, we performed modifications to the input parameters so as to manipulate its value. If we neglect the dependence of the hydrogen recombination coefficient on the temperature, the Strömgren radius R_S is related to the ionizing photon rate $Q(H^0)$, the hydrogen density N_H, and the filling factor ϵ by $R_S \propto (Q(H^0)/N_H^2/\epsilon)^{1/3}$. The ionization parameter at this radius is proportional to $Q(H^0)/N_H/R_S^2$, so we finally have $U \propto (Q(H^0)\, N_H\, \epsilon^2)^{1/3}$.

It is clear that, among the three parameters U depends on, N_H could not be modified because some important nebular lines are sensitive to its value, because of their low critical densities. In the case where U must be increased, changing the filling factor may lead to values $\epsilon > 1$, which is unphysical and not accepted by CLOUDY. Thus, our only possibility of manipulating U was to tune $Q(H^0)$ adequately. However, this supposed an artificial alteration of the line luminosities and of the ionized volume, in proportion to $Q(H^0)$. In the case of the FSp models, it was important to correct the data for this effect, so as to preserve the relative size and luminosity of each individual H II region. Hence, to multiply the ionization parameter by a certain coefficient K for a nebula, we multiplied the spectrum of the ionizing source by K^3 and then divided the output line luminosities and other volume-integrated data by K^3. We checked that this manoeuvre did not cause significant errors (e.g., the Hβ line luminosity was altered by <1%).

3. Models with simple stellar contents

We first investigated models similar to those of EBS07, i.e. with the following parameters: 37 and 56 $M_\odot$ ionizing stars (see Sect. 2.2) and hydrogen density $N_H = 100$ cm^{-3}. However, in contrast to EBS07, we adopted a filling factor $\epsilon = 0.1$, more realistic than $\epsilon = 1$ to describe H II regions.

Along with the CSp and FSp models, we computed models similar to the ones in FSp but with modified stellar spectra to match the ionization parameter of the CSp models, following the method described in Sect. 2.3. We designate those models

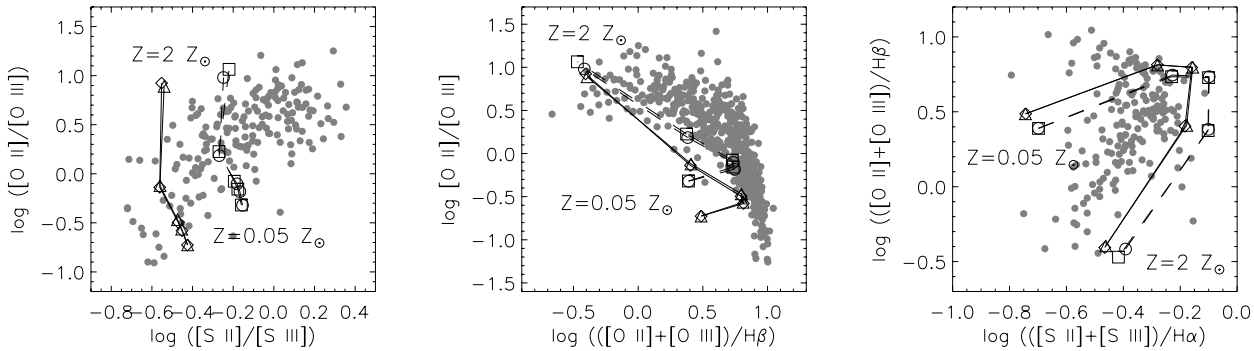

Fig. 1. Comparison of the CSp (full line, diamond symbols), FSp (dashed line, circle symbols), MFSp (full line, triangle symbols), and MCSp (dashed line, square symbols) models computed as in EBS07. The symbols represent the loci of the different metallicities. The metallicities indicated in the diagrams are representative of the points at the ends of the lines they are written close to. The grey circles represent observations made by Garnett et al. (1997), van Zee et al. (1998), Bresolin et al. (1999, 2004, 2005), Kennicutt et al. (2003), and Izotov et al. (2006).

MFSp. The scope of these additional computations was to assess whether the dominant effect of the spatial distribution of the stars was the change in the ionization parameter.

3.1. Results

A comparison between the CSp, FSp, MFSp models is shown in Fig. 1 in the form of four diagrams implying important optical lines (a fourth kind of models, MCSp, is also shown; it is described in Sect. 3.2). In this figure and hereafter, [O II], [O III], [S II], and [S III] refer to [O II]$\lambda\lambda$3726, 3729, [O III]$\lambda\lambda$4959, 5007, [S II]$\lambda\lambda$6716, 6731, and [S III]$\lambda\lambda$9069, 9532, respectively. As it can be seen, the line ratios shown for the CSp and MFSp models are very close to each other, while those of the FSp models are significantly different. We also checked the average temperature values for different ions, defined as:

$$T_0(\mathrm{X}) = \frac{\int N_\mathrm{e}\, N_\mathrm{X}\, \epsilon\, T_\mathrm{e}\, \mathrm{d}V}{\int N_\mathrm{e}\, N_\mathrm{X}\, \epsilon\, \mathrm{d}V} \quad (1)$$

where X is the ion considered, N_X its local density, N_e that of the electrons, and T_e the local electron temperature. We found that, while the temperature discrepancy between the CSp and FSp models reaches up to 8%, it is always less than 1% between the CSp and MFSp cases. This indicates that the variation in the relative intensity of the optical lines with the distribution of the ionizing stars is widely dominated by the variation in U. The contribution of other effects, such as the star-to-star variation in the hardness of the ionizing radiation field, appears to be negligible.

This result suggests the possibility of modeling the effects of the spatial distribution of the stars in a way that does not require a detailed calculation of what occurs around each of those sources. This is what we look into in the next section.

3.2. A simple approximation to the FSp models

As we saw in Sect. 2.3, if we preserve the density and filling factor of a nebula, then we can write the ionization parameter as $U = A\, Q(\mathrm{H}^0)^{1/3}$, where A is a constant[1]. If we call Q_tot the total ionizing rate of a considered cluster, then the ionization parameter for the corresponding CSp model is $U_\mathrm{C} = A\, Q_\mathrm{tot}(\mathrm{H}^0)^{1/3}$. On the other hand, in the case of FSp nebulae, the ionization parameter U_i of each individual H II region i is related to the ionizing photon rate $Q_i(\mathrm{H}^0)$ of its exciting star by $U_i = A\, Q_i(\mathrm{H}^0)^{1/3}$. We can define an average ionization parameter U_F weighted by the coefficients $Q_i(\mathrm{H}^0)$ so as to account for the relative luminosity of each individual nebula:

$$U_\mathrm{F} = \frac{\sum_i Q_i(\mathrm{H}^0)\, U_i}{\sum_i Q_i(\mathrm{H}^0)} \quad (2)$$

$$= A\, \frac{\sum_i Q_i(\mathrm{H}^0)^{4/3}}{Q_\mathrm{tot}(\mathrm{H}^0)} \quad (3)$$

$$= A\, Q_\mathrm{F}(\mathrm{H}^0)^{1/3} \quad (4)$$

with

$$Q_\mathrm{F}(\mathrm{H}^0) = \left(\frac{\sum_i Q_i(\mathrm{H}^0)^{4/3}}{Q_\mathrm{tot}(\mathrm{H}^0)}\right)^3 \quad (5)$$

$$= Q_\mathrm{tot}(\mathrm{H}^0) \left(\sum_i \left(\frac{Q_i(\mathrm{H}^0)}{Q_\mathrm{tot}(\mathrm{H}^0)}\right)^{4/3}\right)^3 . \quad (6)$$

We carried out new calculations with a central source whose spectrum has the same shape as for the total cluster but is normalized to match $Q_\mathrm{F}(\mathrm{H}^0)$. Note that since $U_\mathrm{F} < U_\mathrm{C}$, an equivalent operation would have been to multiply the filling factor ϵ by $(Q_\mathrm{F}(\mathrm{H}^0)/Q_\mathrm{tot}(\mathrm{H}^0))^{1/2}$, which is less than 1. We call these new models "MCSp". At $Z \leq Z_\odot$, the agreement between the FSp and MCSp models is excellent. At $Z = 2\,Z_\odot$, there is greater discrepancy in the intensity of the oxygen lines: the [O II]/Hβ and [O III]/Hβ are larger for FSp models than for MCSp ones by 0.05 and 0.13 dex, respectively. However, the discrepancy for the other lines is less than 0.1 dex.

It appears that, at least within the simple assumptions used in this section (simplified stellar population, constant gas density), tuning the ionization parameter through $Q_\mathrm{tot}(\mathrm{H}^0)$ is sufficient for modeling the effects of the spatial distribution of the ionizing stars quite accurately. This procedure has the significant advantage of requiring only one numerical 1D model, hence representing a huge gain in time over the detailed computation of an FSp model.

4. Models with realistic stellar contents

In the previous section, we explored the effects of the spatial distribution of the ionizing stars making use of a simple stellar

[1] In reality, A is proportional to $\alpha_\mathrm{B}^{2/3}$, where α_B is the case B hydrogen recombination coefficient. The latter depends on the electronic temperature of the gas, T_e (e.g., Péquignot et al. 1991), and we have $A \sim T_\mathrm{e}^{-0.5}$–$T_\mathrm{e}^{-0.6}$. However, in practice, the temperature fluctuations we encountered are small enough to neglect this effect.

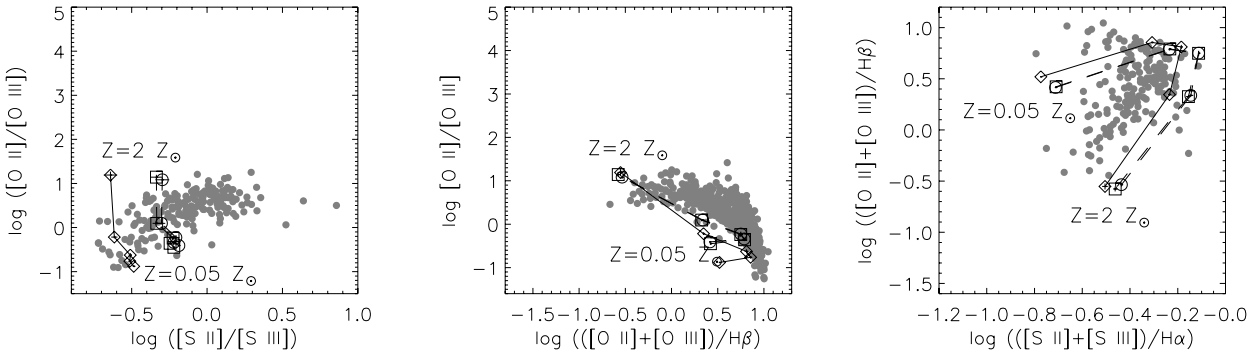

Fig. 2. Comparison of the CSp (full line, diamond symbols), FSp (dashed line, circle symbols), and MCSp (dashed line, square symbols) models computed with random 1 Ma clusters and a density $N_H = 100$ cm^{-3}. Each point corresponds to the average of the 5 simulations computed at the metallicity it represents. The average dispersion between the simulations is reported as error bars on each point. The grey points represent the same observations as in Fig. 1.

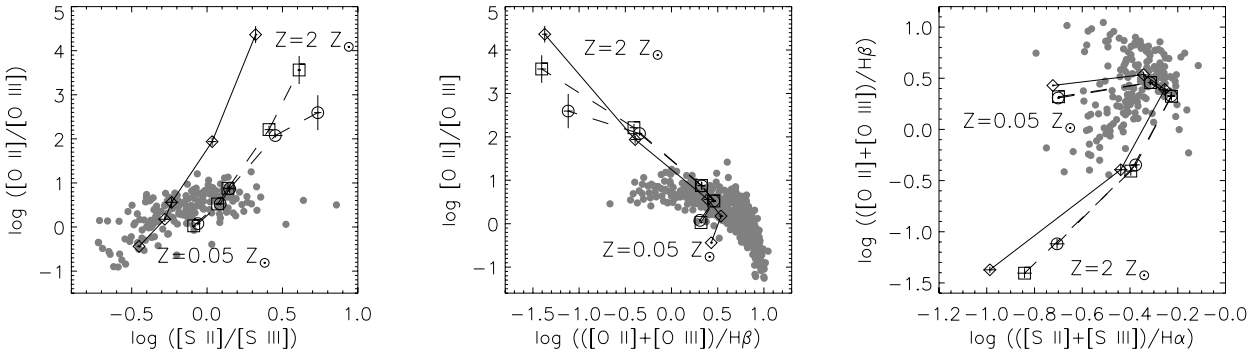

Fig. 3. Same as Fig. 2 but for an age of 4 Ma.

content. It is important to check whether the conclusions of this first approach are still valid if we consider physically realistic stellar clusters, with randomly sampled IMF and ages that are not necessarily as low as 1 Ma. Consequently, we computed new models of nebulae ionized by random clusters (see Sect. 2.2). We considered two gas densities, $N_H = 10$ and 100 cm^{-3}, and two ages, 1 and 4 Ma, while we adopted $\epsilon = 0.1$ in all cases. These two ages were selected because, whereas 1 Ma clusters contain almost exclusively main-sequence (MS) stars, the proportion of post-MS stars and, in particular, of WR ones is significant in 4 Ma old populations. For each age and density, we drew 5 clusters and computed the corresponding CSp, FSp, and MCSp models.

For computational reasons, we used models of moderately massive clusters (with an initial mass of 10^4 $M_\odot$). Many giant H II regions are ionized by more massive populations (e.g., NGC 604: González Delgado & Pérez 2000). On average, the ratio $Q_{tot}(H^0)/Q_F(H^0)$ for a given cluster is proportional to the number of ionizing stars it contains hence to its mass M_{tot} (the exact ratio depends on how the IMF is sampled and on the evolutionary state of the cluster). The ratio U_C/U_F is therefore proportional to $M_{tot}^{1/3}$. Thus, in many cases, the observational properties of giant H II regions will be more sensitive to the distribution of their ionizing stars than our models are.

4.1. Results

In Figs. 2 and 3, we show the results for $N_H = 100$ cm^{-3} and the 1 and 4 Ma clusters, respectively. We do not show the results for $N_H = 10$ cm^{-3} because they are similar to those obtained with $N_H = 100$ cm^{-3} except for a global shift in the emission-line diagnostics, so the comparison between the CSp, FSp, and MCSp models yields the same conclusions at both densities.

In the case of 1 Ma clusters, the agreement between the FSp and MCSp models is excellent at $Z \leq Z_\odot$. At $Z = 2\,Z_\odot$, the discrepancy between both models is slightly larger; however, it does not exceed 0.10 dex for the diagnostics shown in Fig. 2. In the case of 4 Ma clusters, the situation is not that satisfying. Although the FSp and MCSp closely match again at $Z \leq Z_\odot$, they deviate much from each other at $Z = 2\,Z_\odot$, at least regarding the [O III]/Hβ and [O II]/[O III] line ratios. From one simulation to another, the line ratios for both kinds of models tend to shift in the same way, so random variations between the different simulations are not sufficient to explain this discrepancy. Hence, it appears that under certain conditions of age and metallicity, the ionization parameter is not the only important factor in the effects of the dispersion of the ionizing sources, meaning that tuning $Q_{tot}(H^0)$ is not a satisfactory solution when modeling those effects.

5. The FSp/MCSp discrepancy at high ages and metallicities

As we saw in the previous section, the discrepancy observed between the FSp and MCSp models is significant only when both the age and the metallicity of the model objects are high. In this section, we briefly investigate the reasons for this peculiar behavior.

First, let us examine the variety of ionizing continua of the stars in clusters of different ages and metallicities. Given that we

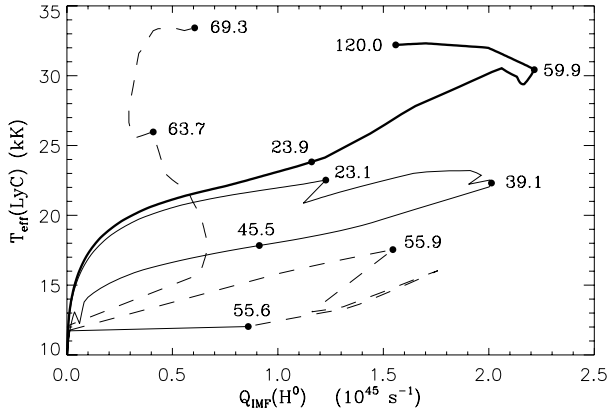

Fig. 4. ($T_{\rm eff}$(LyC), $Q_{\rm IMF}(\rm H^0)$) isochrones for 1 Ma (bold line) and 4 Ma (thin line) stellar populations at $Z = 0.4\ Z_\odot$. The dashed part of the 4 Ma isochrone represents the WR phases. Some initial stellar masses, expressed in $M_\odot$, are reported on the isochrones.

used a Salpeter (1955) IMF, the stars that on average dominate the ionizing flux are those associated to higher values of the following functional:

$$Q_{\rm IMF}(\rm H^0;\ \mathit{M};\ \tau,\ \mathit{Z}) \ = \ (\mathit{M}/\mathit{M}_\odot)^{-2.35}\ \mathit{Q}(\rm H^0;\ \mathit{M};\ \tau,\ \mathit{Z}) \qquad (7)$$

where M is the initial mass of a given star of age τ and metallicity Z, and $Q(\rm H^0;\ M;\ \tau,\ Z)$ its ionizing photon rate. It is also known that, in a pure hydrogen nebula, the energy gain provided by the ionizing source is proportional to the effective temperature of its Lyman continuum:

$$T_{\rm eff}(\rm LyC) \ = \ \frac{2h\nu_0}{3k}\,\frac{\int_{\nu_0}^{+\infty}\frac{L_\nu}{\nu}\left(\frac{\nu}{\nu_0}-1\right)a_\nu\,\mathrm{d}\nu}{\int_{\nu_0}^{+\infty}\frac{L_\nu}{\nu}\,a_\nu\,\mathrm{d}\nu} \qquad (8)$$

where $h\nu_0$ is the hydrogen ionization threshold and a_ν the hydrogen ionization cross-section at frequency ν.

For this reason, we expect that FSp and MCSp models will strongly differ only if stars with high values of $Q_{\rm IMF}(\rm H^0;\ \mathit{M};\ \tau,\ \mathit{Z})$ show a wide range of temperatures $T_{\rm eff}$(LyC). In Fig. 4, we show the ($T_{\rm eff}$(LyC), $Q_{\rm IMF}(\rm H^0)$) isochrones computed for 1 Ma and 4 Ma populations with a metallicity of 0.4 $Z_\odot$. The diagrams at other metallicities are similar to those. As expected, the stars that dominate the ionizing flux show a wider variety of Lyman continua at 4 Ma than at 1 Ma. This explains that the ionization parameter plays the dominant role in the effects of dispersion of the stars in barely evolved clusters. However, physical processes inside the ionized gas are required to explain why the MCSp models only fail to match the FSp ones at high metallicities.

By checking the FSp and MCSp models in detail, we found that their excitation states are very similar (e.g., the $\rm O^{++}/O^{+}$ abundance ratio differs by less than 15% between both cases); however, at the very high metallicity of 2 $Z_\odot$, the abundance of $\rm O^{++}$, an efficient cooling agent in nebulae, is such that the small variation in its abundance between the FSp and MCSp models causes the temperature $T_0(\rm O^{++})$ to vary significantly. This, together with the high sensitivity of the emissivity of the optical [O III] doublet to the temperature in the range considered ($T_0(\rm O^{++}) < 3000$ K), accounts for the FSp/MCSp discrepancy.

Although the FSp/MCSp mismatch analyzed in this section is large, it must be noted that the corresponding models all strongly differ from the comparison data of the surveys we used in this work (see Fig. 3). Unless these surveys are significantly incomplete, our approach to model H II regions with fully distributed ionizing sources therefore applies closely to all observable regimes of age and metallicity.

6. Generalization to other stellar distributions

Despite our success in mimicking the effects of the dispersion of the stars in nebulae with simple models, one should bear in mind the limitations of our work. In particular, we only processed two extreme distributions of the ionizing stars: one where they are all located at one same point, and another where they are separated by distances such that their Strömgren spheres do not overlap.

In the case of a nebula where the Strömgren spheres of its ionizing stars partially overlap, it is probable that adequately tuning the ionization parameter is still a good approximation for treating the distribution of the stars in most cases. However, determining how the average ionization parameter of an H II region depends on the distribution of the stars is a difficult task that may only be solvable through fully three-dimensional modeling. A peculiar case is the one where the distribution of the stars is unknown, e.g. due to the lack of angular resolution. Then, the ionization parameter U used to mimic this distribution becomes a free parameter that should fall within the $U_{\rm F}$–$U_{\rm C}$ interval. The values of both $U_{\rm F}$ and $U_{\rm C}$ depend on the stellar content of the object considered and on the filling factor (see Sect. 2.3). That is, the uncertainty in models of H II regions induced by an unknown distribution of their ionizing stars may be treated by giving some specific margin to the parameters $Q_{\rm tot}(\rm H^0)$ and ϵ.

7. Conclusions

As stated by EBS07, that the ionizing stars of an H II region are spatially dispersed can cause, at least in some cases, its properties to differ quite much from what they would be if all the stars were concentrated in its center. However, they did not study this issue in detail and limited their work to "toy" models of stellar populations. We aimed at assessing whether their conclusions apply to real H II regions of different ages and metallicities. In particular, we were interested in evaluating the importance of the ionization parameter in the way the properties of nebulae depend on the geometry of their ionizing sources. This study was necessary for establishing a technique able to quantify this dependence without requiring heavy calculations.

With this in mind, we ran a series of models using the widespread CLOUDY code, assuming a simple geometry for the ionized gas and two possible distributions of the stars. We found that, in most cases, the variations in the ionization parameter play the dominant role in the differences observed in the nebular diagnostics between the different distributions of the stars. We derived a practical solution to model nebulae where the Strömgren spheres of the stars do not overlap: performing a calculation where the ionizing population remains concentrated in one point but where its absolute spectrum is adequately renormalized. This procedure has the enormous advantage of avoiding any sophisticated modeling, hence saving much computation time (by a factor equal to the number of ionizing stars considered for a given nebula). Moreover, we found only a marginal situation where this solution fails: that of evolved stellar populations (whose ionizing flux is dominated by very different kinds of stars) that ionize a very metal-rich gas cloud. The corresponding models stand far away from the comparative observations

we considered, which minimizes the practical importance of this failure.

An important limit to our approach is that we only considered the two extremes of the possible distributions of the ionizing stars in nebulae: that where all the stars are concentrated in one point and that where each star ionizes a separate part of the available gas. The precise treatment of intermediate distributions is difficult and may be carried out only with fully three-dimensional codes. However, when the distribution of the stars is unknown, it induces an uncertainty in the ionization models that can be easily treated by manipulating the input parameters that are the ionizing rate of the source and the filling factor.

Finally, we only examined models of full sphere nebulae with constant density. Although the generalization to constant density shells should be easy (provided the models with concentrated or distributed stars are well-defined), treating nebulae with spatially variable density cannot be achieved with simple one-dimensional models, since the ionization conditions of each part of a given nebula will depend on the exact position of its ionizing stars. However, our procedure for mimicking the distribution of the ionizing sources may be used as a rough approximation.

Acknowledgements. We are grateful to Grażyna Stasińska for very helpful discussions and comments on this paper. L.J. is supported by a UNAM postdoctoral grant. C.M. is supported by Mexican grants CONACyT 49737 and PAPIIT 115807.

References

Allende Prieto, C., Lambert, D. L., & Asplund, M. 2001, ApJ, 556, L63
Allende Prieto, C., Lambert, D. L., & Asplund, M. 2002, ApJ, 573, L137
Asplund, M. 2000, A&A, 359, 755
Bresolin, F., Kennicutt, R. C., Jr., & Garnett, D. R. 1999, ApJ, 510, 104
Bresolin, F., Garnett, D. R., & Kennicutt, R. C., Jr. 2004, ApJ, 615, 228
Bresolin, F., Schaerer, D., González Delgado, R. M., & Stasińska, G. 2005, A&A, 441, 981
Drissen, L., Roy, J.-R., Robert, C., Devost, D., & Doyon, R. 2000, AJ, 119, 688
Ercolano, B., Barlow, M. J., Storey, P. J., & Liu, X.-W. 2003, MNRAS, 340, 1136
Ercolano, B., Bastian, N., & Stasińska, G. 2007, MNRAS, 379, 945
Ferland, G. J., Korista, K. T., Verner, D. A., et al. 1998, PASP, 110, 761
Garnett, D. R., Shields, G. A., Skillman, E. D., Sagan, S. P., & Dufour, R. J. 1997, ApJ, 489, 63
González Delgado, R. M., & Pérez, E. 2000, MNRAS, 317, 64
Grevesse, N., & Sauval, A. J. 1998, SSRv, 85, 161
Hillier, D. J., & Miller, D. L. 1998, ApJ, 496, 407
Holweger, H. 2001, Joint SOHO/ACE workshop Solar and Galactic Composition, 598, 23
Izotov, Y. I., Stasińska, G., Meynet, G., Guseva, N. G., & Thuan, T. X. 2006, A&A, 448, 955
Kennicutt, R. C., Jr., Bresolin, F., & Garnett, D. R. 2003, ApJ, 591, 801
Leitherer, C., Schaerer, D., Goldader, J. D., et al. 1999, ApJS, 123,
Lejeune, T., Cuisinier, F., & Buser, R. 1997, A&AS, 125, 229
Meynet, G., Maeder, A., Schaller, G., Schaerer, D., & Charbonnel, C. 1994, A&AS, 103, 97
Pauldrach, A. W. A., Hoffmann, T. L., & Lennon, M. 2001, A&A, 375, 161
Péquignot, D., Petitjean, P., & Boisson, C. 1991, A&A, 251, 680
Salpeter, E. E. 1955, ApJ, 121, 161
Smith, L. J., Norris, R. P. F., & Crowther, P. A. 2002, MNRAS, 337, 1309
van Zee, L., Salzer, J. J., Haynes, M. P., O'Donoghue, A. A., & Balonek, T. J. 1998, AJ, 116, 2805